

**CHEMICAL PROCESS EFFECTS ON SLOPED SURFACE WITH  
CHANGING MASS AND CONSISTENT TEMPERATURE**

Nagarajan Gnanavel<sup>1</sup>, SundarRaj Mariadoss<sup>1\*</sup>, Venkatesan Jayavelu<sup>2</sup>, Venkata  
MohanReddy Polaka<sup>3</sup>, Muthucumaraswamy Rajamanickam<sup>4</sup>

<sup>1</sup>Department of Mathematics, Panimalar Engineering College, Poonamallee, Chennai  
600123, Tamil Nadu, India

<sup>2</sup>Department of Mathematics, Rajalakshmi Engineering College, Thandalam, Chennai  
602105

<sup>3</sup>Department of Science and Humanities, R.M.D. Engineering College, Kavaraipettai  
601206, India,

<sup>4</sup>Department of Applied Mathematics, Sri Venkateswara College of Engineering,  
Sriperumbudur 602117, Tamil Nadu, India

<https://doi.org/10.2298/CICEQ231212023G>

**Received 12.12.2023.**

**Revised 30.5.2024.**

**Accepted 13.6.2024.**

---

\* Correspondence: Dr. M. Sundar Raj, Department of Mathematics, Panimalar Engineering College, Chennai-  
600123, India. Email:[sundarrajkani@gmail.com](mailto:sundarrajkani@gmail.com)

## **Abstract**

The research extensively investigated the turbulent flow patterns surrounding an unbounded inclined plate under the conditions of uniform temperature and variable mass dispersion. Throughout this analysis, the study thoroughly considered the impact of chemical reactions within the system. Focusing on the harmonic inclination of the plate within its plane, the study employed the LT approach to accurately solve the non-dimensional governing equations. In scrutinizing various profiles, the investigation examined the impact of several crucial physical factors: chemical response variable, Schmidt number, thermal Grashof number, mass Grashof number, and duration. This study delves into the intricate influence of various factors on the complex flow dynamics surrounding inclined plates, specifically focusing on heat and mass transfer phenomena. By examining these relationships, the research provides crucial insights into improving the efficiency of thermal and mass transmission processes within systems that incorporate tilted surfaces. Moreover, this knowledge can potentially contribute to advancements in various fields, from renewable energy systems to manufacturing processes, where heat and mass transfer play pivotal roles.

**Keywords:** tilted surface; thermal transfer; mass transmission; chemical reaction; Laplace transform method.

### **Highlights:**

- Velocity escalates during generative reactions but diminishes during destructive reactions.
- Chemical reaction parameter decrease correlated with increased velocity.
- Variables relate to local skin friction, impacting frictional forces over time.
- Sherwood number ties to material transmission, shaping dynamics over time.
- The dimensionless governing equations were tackled using the Laplace transform method.

## INTRODUCTION

In numerous industrial and engineering contexts, the utilization of synthetic response impacts on a continuously propelled inclined surface characterized by variable material dispersion and uniform temperature can be advantageous. Chemical Vapor Deposition (CVD) is extensively used in semiconductor manufacturing whose process involves the deposition of thin films on substrates. By comprehending the synthetic response influences on an inclined surface characterized by varying material dispersion, the CVD process can be optimized to produce films of higher quality and greater uniformity. In the pharmaceutical industry and drug manufacturing, certain reactions require precise control of temperature and mass diffusion. The study of chemical reactions on an inclined plate can contribute to optimizing reaction conditions for pharmaceutical synthesis. The design of chemical reactors involves controlling temperature gradients and mass diffusion for efficient chemical transformations. Chemical reactions occurring on a slanted surface with changeable material dispersion may yield information that can be utilized to improve reactor design. In surface coating processes industries such as automotive or aerospace, the coating processes are crucial. Understanding how chemical reactions affect the coating on a linearly accelerated inclined plate can enhance the quality and durability of the coatings.

The environmental engineering studies of chemical reactions on an inclined plate have many applications, particularly in processes related to air and water purification. This knowledge can aid in designing efficient systems for pollutant removal. Food processing applications involving certain processing techniques involve chemical reactions. For example, understanding the effects of an inclined plate can contribute to optimizing processes like drying or frying in the food industry. Chemical reactions occur at the electrode surfaces in energy storage systems in the development of batteries or fuel cells. Research on inclined plates can provide insights into optimizing reaction conditions for improved energy storage and conversion efficiency. Understanding the chemical reactions on an inclined plate is relevant to material synthesis. This knowledge can be applied to develop advanced materials with tailored properties for specific applications, such as in the aerospace or electronics industry. The study of chemical reactions on inclined plates can have applications in areas such as drug delivery systems or bioengineering processes in biomedical applications and medical research. Also, the chemical reactions on inclined

plates can be relevant in designing systems for treating industrial waste and optimizing the removal of pollutants through controlled reactions.

Bég et al. [1] examined numerical methods that accounted for the Soret and Dufour influences in mixed convective conditions while investigating heat and mass transfer in dynamically reactive flows along angled as well as perpendicular surfaces. Using magnetohydrodynamics (MHD), Orhan Aydm and Ahmet Kaya [2] examined the combined convection thermal flow surrounding an angled surface. The influence of magnetohydrodynamics (MHD) on a vertically oscillating plate during a 1st level synthetic response was investigated by Muthucumaraswamy et al. [3]. In a study by Muthucumaraswamy [4], the examination focused on the impacts of chemical reactions on fluid flow over a vertical plate that oscillates while maintaining uniform mass diffusion at different temperature levels. Bisht et al. [5] examined the impact of elemental responses and varying heat conductance on the outer region movement of constant combined convective flows, which involved thermal as well as material transmission inside a tapered shape and was propelled by an area basin. The investigation carried out by SundarRaj et al. [6] analyzed magnetohydrodynamic convective flow around an accelerated, isothermal vertical plate featuring variable mass diffusion. Makinde [7] conducted an in-depth investigation into the vacillating circulation of radiating liquid undergoing chemical reactions and subjected to hydromagnetic influences. The study focused on the fluid dynamics around a perpendicular exterior with consistent thermal fluctuation. Puneet Rana et al. [8] examined a mathematical model for the combined convective barrier layered movement of a minuscule level liquid across a permeable intermediate-positioned slanted surface. The investigation probed the intricacies of heat and mass transfer phenomena. Mohammad Shah Alam et al. [9] conducted an extensive study on the HMT phenomena in magnetohydrodynamic unrestricted convection circulation across a tilted surface, incorporating the influence of Hall current. The research aimed to unravel the intricacies of the thermal and mass transport characteristics in this specific configuration. Muthucumaraswamy and Jeyanthi [10] conducted an extensive study on the Hall effects influencing the magnetohydrodynamic (MHD) flow over an infinite vertical plate. This investigation involved a rotating fluid with variable temperature and mass diffusion, along with the inclusion of a first-order chemical reaction.

Narahari et al. [11] explored the intricate dynamics of unsteady magnetohydrodynamic unrestricted convective circulation across a boundless tilted surface. The investigation considered the impact of sloped circumstances and incorporated emission, thermal origins,

and synthetic responses. The research aimed to provide a comprehensive understanding of the total influences of these parameters on the circulation factors and HMT phenomena. Mondal et al. [12] delved into the intricate aspects of magnetohydrodynamic combined convective material transmission across a tilted surface. Inconsistent thermal factors and the impact of synthetic responses were taken into consideration in the study. The primary objective of the study was to attain an in-depth knowledge of the intricate relationship among these phenomena and how they impact the processes of material transmission across the tilted surface. Farjana et al. [13] presented a numerical investigation of boundary layer mass transfer flow over an inclined plate, considering the effects of chemical reaction and thermal diffusion. An analysis of unsteady MHD free convection flow oriented heat and mass transfer past an exponentially accelerated inclined plate embedded in a saturated porous medium with uniform permeability, variable temperature, and concentration has been studied by Rani Pattnaik et al.[14]

Khalid et al. [15] conducted an investigation into the merged influences of buoyancy along with synthetic responses on the magnetohydrodynamic flow of Casson liquids across a permeable context. The study focused on the flow dynamics induced by a porous shrinking sheet. The research enabled an understanding of the interactions between buoyancy, chemical reactions, and the unique characteristics of Casson fluids near a permeable shrinking sheet. Sailaja et al. [16] analyzed the influence of twin divergent influences in magnetohydrodynamic combined convective flow across a perpendicular tilted surface. The study considered the existence of a permeable environment and incorporated the Biot number as a parameter. The research employed a finite element technique to analyze the complex interactions within this system. The aim was to gain a comprehensive understanding of the impact of double diffusive effects on the flow dynamics of specific liquids near a permeable environment and a vertically inclined plate considering numerous factors.

Dhal et al. [17] explored the impacts of HMT on magnetohydrodynamic unrestricted convective circulation across a tilted and numerically expedited surface fixed in a permeable environment having a thermal intake. The study aimed to understand the complex interactions between HMT phenomena near MHD effects, an inclined plate, exponential acceleration, and a permeable environment with a heat source. Rajput and Gaurav Kumar [18] investigated the influence of element responses on the unstable magnetohydrodynamic circulation across a uniform expedited tilted surface. The study considered varying degrees, material dispersion, etc. The research aimed to

comprehensively understand the influence of chemical reactions on the circulation dynamics amidst varying temperatures, mass diffusion, and Hall current. Suman Agarwalla and Nazibuddin Ahmed [19] conducted a study on the magnetohydrodynamic material transmission circulation across a tilted surface having varying temperatures as well as surface pace. The investigation considered the plate to be fixed in a permeable environment. The research aimed to gain insights into the complex interactions of MHD effects, mass transfer, variable temperature, plate velocity, and the impact of a permeable environment on the circulation characteristics around the inclined plate. Hiranmoy Mondal et al. [20] initiated a comprehensive investigation on the influence of thermal parameters in a magnetohydrodynamic mixed convective material transmission across a tilted surface. The research incorporated inconsistent thermal impacts and considered the influence of chemical reactions. The study aimed to provide a comprehensive understanding of the intricate interplay between thermophoresis, and Soret-Dufour effects on the material transmission parameters over the inclined plate. Ahmad et al. [21] conducted a proportional investigation of the unrestricted convective circulation of magnetohydrodynamic liquid. The investigation considered a heat source and a 1<sup>st</sup> level synthetic response. The research aimed to comprehensively analyze and compare the dynamics of natural convection in non-Newtonian fluids influenced by MHD effects and heat sources.

Sandhya et al. [22] analyzed the influences of HMT on magnetohydrodynamic circulation across a tilted permeable surface amidst synthetic responses. The investigation evaluated the mixed influences of MHD, HMT, and chemical reactions on the circulation parameters near an inclined porous plate. Oyekunle and Agunbiade [23] conducted a study on the influences of various parameters near an inclined magnetic field, on the magnetohydrodynamic circulation across a perforated perpendicular surface. The research evaluated the interplay of these factors on the dynamics of the unpredictable MHD slippage circulation across a perforated perpendicular surface, particularly considering the inclined magnetic field. Thamizh Suganya et al. [24] examined the sensitivity of factors in magnetohydrodynamic unconstrained turbulent circulation across an angled surface through a statistical analysis. The objective of the research was to conduct a thorough analysis and discourse on the mechanics of unconstrained convective circulation in MHD, with a particular focus on sloped surfaces. Sensitivity analyses were also performed on a range of influential parameters. Idowu and Falodun [25] explored the effects of thermophoresis and Soret-Dufour on the heat and mass transfer flow of magnetohydrodynamics non-Newtonian nanofluids over an inclined plate. The study explored the impact of these phenomena on the

HMT parameters in the presence of magnetohydrodynamics and, an inclined plate. Riaz et al. [26] examined the unconstrained convective circulation of magnetohydrodynamics over an upward surface, taking into account scaled thermal levels, synthetic responses, and particle factors. The investigation evaluated the interplay of these factors on the circulation characteristics over a perpendicular surface.

A probability investigation was performed by Praveen Kumar Dadheech et al. [27] on radiative inclined magnetohydrodynamic slip circulation with a thermal origin in a permeable environment, taking into account 2 distinct liquids. The research explored entropy variations in the context of radiative inclined MHD slip flow with a heat source, particularly for two distinct fluids within a porous medium. The convective movement of a fluid over an angled surface was investigated by Azhar Ali Zafar et al. [28] in the presence of thermal along with matter movement. The study evaluated the dynamics of free-convection flow influenced by magneto hydrodynamics. Utilizing mathematical techniques, Darapuneni Purna Chandra Rao et al. [29] examined the features of liquid circulation. The research was centered on the Darcy-Forchheimer movement of a Ree-Eyring liquid throughout an angled surface, with organic processes factored into consideration. Raghunath et al. [30] investigated the dynamics of magnetohydrodynamic fluid flow. The study focused on an inclined vertical porous plate under unsteady conditions, considering the impact of various parameters. The influence of HMT on the velocity of a magnetohydrodynamic Casson solution was examined by Vijayaragavan et al. [31]. The study specifically considered the presence of an inclined plate. The influence of heat dispersion and an angled magnetic environment on the unimpeded convective circulation of Casson liquid was examined by Pavan Kumar et al. [32]. The research explored the interaction of different variables with an angled surface within an electrical environment. The impact of emission, diffusive heat, organic responses, and erratic spontaneous convection around an angled perpendicular surface was investigated by Suresh Babu et al. [33], with a specific focus on the consequences of oriented magnetization. Raghunath Kodi and Obulesu Mopuri [34] analyzed the unsteady hydrodynamic flow over an inclined plate embedded in a porous medium, considering a Soret-aligned magnetic field and chemical reaction.

Using the Galerkin FEM, Shankar Goud Bejawada et al. [35] examined the movement characteristics of a magnetized tiny liquid with molecular reaction and inertial dispersion. An investigation was conducted by Husna Izzati Osman et al. [36] regarding unconstrained vortex movement in the vicinity of an infinitely slanted surface. In their

investigation, Tad and Ahmed [37] examined the unimpeded convective circulation of MHD across a slanted permeable surface. They took into account various factors including the thermal origin, Soret impact, organic response, sticky dissolution, as well as electromagnetic warming. The influence of heat diversification on circulation within an angled rapid segmented surface with uninterrupted material dispersion was examined by Nagarajan et al. [38].

Bang Chuol Nhial et al. [39] investigated the effects of material transmission and radioactivity on magnetohydrodynamic (MHD) unconstrained circulation across an angled surface. The mechanics of unstable magnetohydrodynamic liquid circulation over a tilted orthogonal perforated surface were investigated by Kodi Raghunath et al. [40]. In addition to emission, synthesized reactions, and synchronized electromagnetic areas, the investigation examined the possibility of Soret impacts. Mohana Ramana et al. [41] examined the effects of an oriented magnetic environment as well as organic processes on the erratic MHD Kuvshinski liquid circulation across an angled perforated surface. The investigation also analyzed the existence of emissions and other influences. Nasir Shehzad et al. [42] examined the impact of magnetohydrodynamics movement on multiple layers within a permeable slanted rotational conduit employing either conventional as well as unconventional liquids. Ali Raza and colleagues [43] researched magnetohydrodynamics in the context of an inclined face. The introduction of nanofluids through conventional heat methods was crucial to their research. An investigation was undertaken by Sivakumar and Muthucumaraswamy [44] to examine the impact of emissions on the conical circulation encircling a perpendicular infinitely homogeneous surface. Additionally, chemical reaction influences and progressively enhanced material dispersion were accounted for in the investigation. The mechanics of erratic magnetohydrodynamic cyclical Casson liquid circulation across an angled perpendicular permeable surface were explored by Raghunath and Mopuri [45]. The study included considerations for chemical reactions, heat absorption, and Soret effects. Sundar Raj et al. [46] examined the impact of chemical reactions on an inclined isothermal vertical plate. The study delved into the velocity profile under various conditions of  $T_H$ ,  $T_G$ , and  $Sc$ . Nur Syahirah Wahid et al. [47] examined the behavior of a magnetohydrodynamic combination of tiny liquids by combined flow over a decreasing porous slanted surface, taking into account the impact of heat emission. J.S. Huang [48] investigated the heat and mass transfer in a fluid undergoing convective flow along an inclined plate through a porous medium, considering the effects of chemical reaction and activation energy. Prabhakar Reddy et al. [49] conducted a finite difference computational

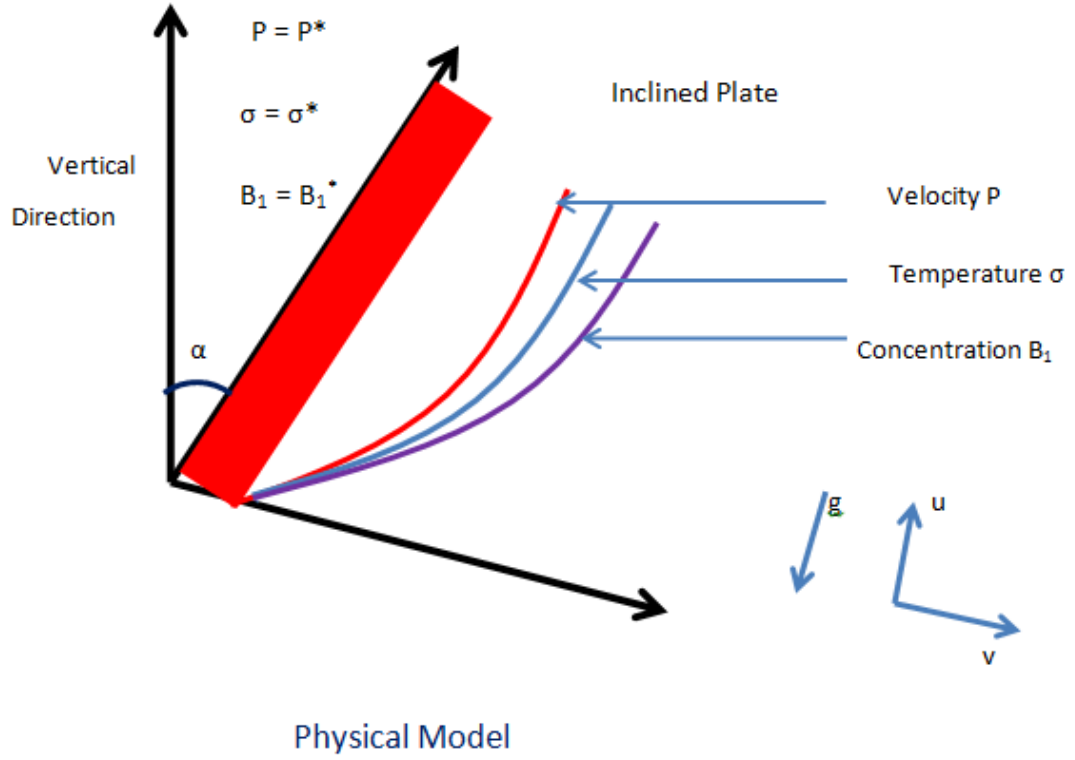


study to evaluate the influence of thermal diffusion and chemical reaction on unsteady free convective radiative magnetohydrodynamic flow past an exponentially accelerated inclined permeable plate. This study considered a plate embedded in a saturated porous medium of uniform permeability with variable temperature and concentration. K. V. Raju et al. [50] examined the unsteady MHD flow of an incompressible water-based Jeffrey nanofluid (containing Cu and TiO<sub>2</sub>) across a stretched sheet in a transverse magnetic field, taking into account thermal radiation and Soret effects. Rajaraman and Muthucumaraswamy [51] have investigated the impact of chemical reactions, viscous dissipation, and thermal radiation on MHD flow past an oscillating plate.

No experts have yet offered a quantitative exploration into how chemical reactions impact an unsteady linearly accelerated inclined plate with uniform temperature and variable mass diffusion. Consequently, this present study aims to examine the influence of chemical reactions on such a scenario of a linearly accelerated inclined plate with uniform temperature and variable mass diffusion. The study used the Laplace transform approach to precisely solve the non-dimensional governing equations.

## ANALYSIS

When examining the irregular motion of a viscous fluid as it passes over a surface that is constantly inclined in a straight line and protrudes at an offset to the vertical plane. While the x-orientation axis is aligned transverse to the straight surface, the y-orientation is aligned parallel to it. While  $t_3^* \leq 0$  the surface as well as liquid subsist at consistent temperatures  $F_\infty^*$ . While  $t_3^* > 0$  the surface is accelerated  $u = u_0 t_3^*$  inside its surface, its degree is elevated  $N_w^*$ . The material is moved from the surface to the fluid. Successive compositions employing traditional Boussinesq's assumption thus govern the irregular movement. The geometrical model of the problem is shown below.



$$\frac{\partial u}{\partial t_3^*} = g \cos \alpha^* (F^* - F_\infty^*) \beta_2 + g \cos \alpha^* (N^* - N_\infty^*) \beta_2^* + \nu \frac{\partial^2 u}{\partial y^2}$$

$$\rho C_p \frac{\partial F^*}{\partial t_3^*} = k \frac{\partial^2 F^*}{\partial y^2} \quad (1)$$

$$\frac{\partial N^*}{\partial t_3^*} = D \frac{\partial^2 N^*}{\partial y^2} - K_l N^*$$

At initial as well as circumferential circumstances:

$$\begin{aligned} u = 0, \quad F^* = F_\infty^*, \quad N^* = N_\infty^* \quad \text{for all } y, t_3^* \leq 0 \\ t_3^* > 0: \quad u = u_0 t_3^*, \quad F^* = F_w^*, \quad N^* = N_w^* \quad \text{at } y = 0 \\ u \rightarrow 0 \quad F^* \rightarrow F_\infty^*, \quad N^* \rightarrow N_\infty^* \quad \text{as } y \rightarrow \infty \end{aligned} \quad (2)$$

Here,  $A = \left( \frac{u_0^2}{\nu} \right)^{\frac{1}{3}}$ .

Upon the presentation of the pertinent devoid of dimension factors:

$$P_2^* = \frac{u}{(vu_0)^{\frac{1}{3}}}, t = t_3 \left( \frac{u_0^2}{v} \right)^{\frac{1}{3}}, Y = y \left( \frac{u_0}{v^2} \right)^{\frac{1}{3}}, K_2^* = K_l \left( \frac{v}{u_0^2} \right)^{\frac{1}{3}},$$

$$\sigma^* = \frac{F^* - F_\infty^*}{F_w^* - F_\infty^*}, Gr = \frac{g\beta_2(F_w^* - F_\infty^*)}{u_0}, B_1^* = \frac{N_\infty^* - N_w^*}{N_w^* - N_\infty^*}, \quad (3)$$

$$Gc = \frac{g\beta_2^*(N_w^* - N_\infty^*)}{u_0}, Pr = \frac{\mu C_p}{k}, sc = \frac{v}{D}$$

Eqs. (1) and (4), results in

$$\frac{\partial P^*}{\partial t} = \sigma^* Gr \cos \alpha^* + B_1^* Gc \cos \alpha^* + \frac{\partial^2 P_2^*}{\partial Y^2}$$

$$\frac{\partial \sigma^*}{\partial t} = \frac{1}{Pr} \frac{\partial^2 \sigma^*}{\partial Y^2} \quad (4)$$

$$\frac{\partial B_1^*}{\partial t} = \frac{1}{sc} \frac{\partial^2 B_1^*}{\partial Y^2} - K_2^* B_1^*$$

Regarding non-dimensional factors, the initial and final restrictions were

$$P_2^* = 0, \quad \sigma^* = 0, \quad B_1^* = 0 \quad \text{for all } Y, t \leq 0$$

$$t > 0: \quad P_2^* = t, \quad \sigma^* = 1, \quad B_1^* = t \quad \text{at } Y = 0$$

$$P_2^* \rightarrow 0, \quad \sigma^* \rightarrow 0, \quad B_1^* \rightarrow 0 \quad \text{as } Y \rightarrow \infty \quad (5)$$

## SOLUTION

We apply the Laplace transform to both sides of the dimensionless arithmetic statements in equation (4), ensuring they comply with the threshold requirement specified in equation (5)

$$\sigma^* = \text{erfc} \left( Z_2^* \sqrt{\text{Pr}} \right) \quad (6)$$

$$\begin{aligned}
B_1^* = & \frac{t}{2} \left[ \exp(2Z_2^* \sqrt{K_2^* t sc}) \operatorname{erfc}(Z_2^* \sqrt{sc} + \sqrt{K_2^* t}) \right. \\
& \left. + \exp(-2Z_2^* \sqrt{K_2^* t sc}) \operatorname{erfc}(Z_2^* \sqrt{sc} - \sqrt{K_2^* t}) \right] \\
& - \frac{z_2^* \sqrt{sc} t}{2\sqrt{K^*}} \left[ \exp(-2Z_2^* \sqrt{K_2^* t sc}) \operatorname{erfc}(Z_2^* \sqrt{sc} - \sqrt{K_2^* t}) \right. \\
& \left. - \exp(2Z_2^* \sqrt{K_2^* t sc}) \operatorname{erfc}(Z_2^* \sqrt{sc} + \sqrt{K_2^* t}) \right]
\end{aligned} \tag{7}$$

$$\begin{aligned}
P_2^* = & \left( 1 - d - \frac{b}{c(1-sc)} \right) t \left[ \left( 1 + 2Z_2^{*2} \operatorname{Pr} \right) \operatorname{erfc}(Z_2^*) - \frac{2Z_2^*}{\sqrt{\pi}} e^{-Z_2^{*2}} \right] - \frac{b}{c^2(1-sc)} \operatorname{erfc}(Z_2^*) \\
& - \frac{b e^{ct}}{2c^2(1-sc)} \left[ \exp(2Z_2^* \sqrt{ct}) \operatorname{erfc}(Z_2^* + \sqrt{ct}) + \exp(-2Z_2^* \sqrt{ct}) \operatorname{erfc}(Z_2^* - \sqrt{ct}) \right] \\
& + d t \left[ \left( 1 + 2Z_2^{*2} \operatorname{Pr} \right) \operatorname{erfc}(Z_2^* \sqrt{\operatorname{Pr}}) - \frac{2Z_2^* \sqrt{\operatorname{Pr}}}{\sqrt{\pi}} e^{-Z_2^{*2} \operatorname{Pr}} \right] \\
& - \frac{b}{2c^2(1-sc)} \left[ \exp(2Z_2^* \sqrt{K_2^* t sc}) \operatorname{erfc}(Z_2^* \sqrt{sc} + \sqrt{K_2^* t}) \right. \\
& \left. + \exp(-2Z_2^* \sqrt{K_2^* t sc}) \operatorname{erfc}(Z_2^* \sqrt{sc} - \sqrt{K_2^* t}) \right] \\
& - \frac{bt}{2c(1-sc)} \left[ \exp(2Z_2^* \sqrt{K_2^* t sc}) \operatorname{erfc}(Z_2^* \sqrt{sc} + \sqrt{K_2^* t}) \right. \\
& \left. + \exp(-2Z_2^* \sqrt{K_2^* t sc}) \operatorname{erfc}(Z_2^* \sqrt{sc} - \sqrt{K_2^* t}) \right] \\
& + \frac{bz_1^* \sqrt{t sc}}{2c\sqrt{K^*}(1-sc)} \left[ \exp(2Z_2^* \sqrt{K_2^* t sc}) \operatorname{erfc}(Z_2^* \sqrt{sc} + \sqrt{K_2^* t}) \right. \\
& \left. + \exp(-2Z_2^* \sqrt{K_2^* t sc}) \operatorname{erfc}(Z_2^* \sqrt{sc} - \sqrt{K_2^* t}) \right] \\
& + \frac{dt^2}{6} \left[ \left( 3 + 12Z_2^{*2} \operatorname{Pr} + 4Z_2^{*4} \operatorname{Pr}^2 \right) \operatorname{erfc}(Z_2^* \sqrt{\operatorname{Pr}}) - \frac{Z_2^* \sqrt{\operatorname{Pr}}}{\sqrt{\pi}} \left( 10 + 4Z_2^{*2} \operatorname{Pr} \right) e^{-Z_2^{*2} \operatorname{Pr}} \right] \\
& + e_1 \frac{e^{ct}}{2} \left[ \exp(2Z_2^* \sqrt{sc(K_2^* + c)t}) \operatorname{erfc}(Z_2^* \sqrt{sc} + \sqrt{(K_2^* + c)t}) \right. \\
& \left. + \exp(-2Z_2^* \sqrt{sc(K_2^* + c)t}) \operatorname{erfc}(Z_2^* \sqrt{sc} - \sqrt{(K_2^* + c)t}) \right] \\
& - \frac{e_1}{2} \left[ \exp(2Z_2^* \sqrt{K_2^* t sc}) \operatorname{erfc}(Z_2^* \sqrt{sc} + \sqrt{K_2^* t}) + \exp(-2Z_2^* \sqrt{K_2^* t sc}) \operatorname{erfc}(Z_2^* \sqrt{sc} - \sqrt{K_2^* t}) \right]
\end{aligned}$$

$$-\frac{be^{ct}}{2c^2(1-sc)} \left[ \exp(2Z_2^* \sqrt{(K_2^*+c)tsc}) \operatorname{erfc}(Z_2^* \sqrt{sc} + \sqrt{(K_2^*+c)t}) \right. \\ \left. + \exp(-2Z_2^* \sqrt{(K_2^*+c)tsc}) \operatorname{erfc}(Z_2^* \sqrt{sc} - \sqrt{(K_2^*+c)t}) \right] \quad (8)$$

Where,  $a = Gr \cos \alpha^*$ ,  $b = Gc \cos \alpha^*$ ,  $c = \frac{K_2^* sc}{1-sc}$ ,  $d = \frac{a}{1-Pr}$ ,  $Z_2^* = \eta = \frac{Y}{2\sqrt{t}}$

### Skin Friction

The non-dimensional plate friction factor seems to be

$$\tau = - \left( \frac{\partial P_2^*}{\partial y} \right)_{y=0}$$

$$\tau = 2(1-d + cbe_1 + e_1) \sqrt{\frac{1}{\pi}} + dt \left( -2\sqrt{\frac{pr}{\pi}} \right) - \frac{e_1 e^{ct}}{2} \left[ \sqrt{c} \operatorname{erfc}(\sqrt{ct}) - \frac{2e^{-ct}}{\sqrt{\pi}} - \sqrt{c} \operatorname{erfc}(\sqrt{ct}) \right]$$

$$- \frac{e_1}{2} \left[ -2\sqrt{\frac{sc}{\pi t}} e^{-K_2^* t} + \sqrt{K_2^* sc} \left( \operatorname{erfc}(\sqrt{K_2^* t}) - \operatorname{erfc}(-\sqrt{K_2^* t}) \right) \right]$$

$$+ \frac{e_1 \sqrt{sc}}{4\sqrt{K_2^*}} \left( \operatorname{erfc}(-\sqrt{K_2^* t}) - \operatorname{erfc}(\sqrt{K_2^* t}) \right)$$

$$- \frac{ce_1 \sqrt{t}}{4} \left[ -2\sqrt{\frac{sc}{\pi t}} e^{-K_2^* t} + \sqrt{K_2^* sc} \left( \operatorname{erfc}(\sqrt{K_2^* t}) - \operatorname{erfc}(-\sqrt{K_2^* t}) \right) \right]$$

$$- \frac{e_1 e^{ct}}{4\sqrt{t}} \left[ -4\sqrt{\frac{sc}{\pi}} e^{-(K_2^*+c)t} + 2\sqrt{sc(K_2^*+c)t} \left( \operatorname{erfc}(\sqrt{(K_2^*+c)t}) - \operatorname{erfc}(-\sqrt{(K_2^*+c)t}) \right) \right] \quad (9)$$

Where  $e_1 = \frac{b}{c^2(1-sc)}$

## Sherwood number (Sh)

Sh is given by

$$Sh = - \left( \frac{\partial B_1^*}{\partial y} \right)_{y=0}$$
$$Sh = - \frac{\sqrt{t}}{4} \left[ 2\sqrt{K_2^* t sc} \operatorname{erfc}(\sqrt{K_2^* t}) - \frac{2\sqrt{sc}}{\sqrt{\pi}} e^{-K_2^* t} - 2\sqrt{K_2^* t sc} \operatorname{erfc}(-\sqrt{K_2^* t}) - \frac{2\sqrt{sc}}{\sqrt{\pi}} e^{-K_2^* t} \right]$$
$$+ \frac{\sqrt{t sc}}{4\sqrt{K_2^*}} \left[ \operatorname{erfc}(-\sqrt{K_2^* t}) - \operatorname{erfc}(\sqrt{K_2^* t}) \right]$$
(10)

## Nusselt number (Nu)

Nu is given by

$$Nu = - \left( \frac{\partial \sigma^*}{\partial y} \right)_{y=0}$$
$$Nu = \sqrt{\frac{pr}{\pi t}}$$
(11)

## RESULTS AND DISCUSSION

To attain a more comprehensive comprehension of the issue at hand, analytical formulas were used to examine the fluctuations in speed, heat, and composition. A variety of mathematical variables, including the slope direction, molecular response variable, heat and material differential values, Sc, Pr, and t, were utilized in these calculations. All of these variables significantly influence the characteristics of movement as well as transportation processes that occur inside an environment that incorporates water vapor as well as airflow.

The solutions derived through Laplace transforms are written concerning exponential functions and complementary error functions. These mathematical representations provide a framework to comprehend how these parameters intricately influence various parameters. They offer valuable insights into the collective impact of these parameters on the dynamics of flow and transport.

Figure 1 demonstrates how concentration profiles change over time for different values of the chemical reaction parameter  $K_2^*$ . The graph shows a decrease in wall concentration due to chemical reactions occurring within the system.

Figure 1

Figure 2 illustrates how velocity profiles change over different time intervals, showing a consistent increase in velocity as time passes. This gradual acceleration in velocity suggests a dynamic shift within the system, with velocities steadily rising over time. These observations provide valuable insights into how the system evolves temporally, shedding light on how flow dynamics change with time. This trend underscores the system's responsiveness, demonstrating how velocities evolve and potentially escalate as the study progresses. Recognizing the connection between velocity and time is crucial for grasping the system's transient nature and understanding how flow dynamics evolve.

This progressive increment in velocity over time signifies an evolving dynamic within the system. Such insights into the temporal evolution of velocity profiles are crucial for understanding the system's behavior and the change of flow dynamics concerning time. This trend highlights the system's response, showcasing how velocities evolve and potentially intensify as the temporal aspect of the study progresses. Understanding this relationship between velocity and time is essential for comprehending the system's transient behavior and the temporal evolution of flow dynamics.

Figure 2

In Figure 3, the visualization illustrates the influence of velocity across various contexts. The diagram demonstrates a trend where velocity increases as the CRP (Chemical Reaction Parameter) decreases. This observed relationship highlights an essential aspect of the system's behavior, suggesting that lower reaction parameter values are associated with higher velocities. This indicates a possible inverse relationship between the chemical reactions occurring in the system and the resulting flow dynamics. Understanding this trend

offers valuable insights into how changes in the reaction parameter distinctly affect and potentially control the speed patterns within the studied environment.

This observed relationship between the velocity and the reaction parameter signifies a crucial aspect of the system's behavior. It suggests that lower values of the reaction parameter correspond to heightened velocities, indicating a potentially inverse relationship between chemical reactions occurring in the system and the resulting flow dynamics. Understanding this trend provides valuable insights into how variations in the reaction parameter distinctly influence and potentially modulate the speed contours within the studied environment.

### Figure 3

Figure 4 illustrates the velocity patterns for various Grashof numbers ( $Gr$ ). In both figures, a clear trend is evident: as the Grashof number increases, the velocity within the system rises significantly. This pattern underscores the considerable impact of the Grashof number on flow dynamics across different inclinations. Grasping this correlation is vital for understanding how changes in the Grashof number distinctly influence and potentially control flow behaviors within diverse system configurations and inclinations.

This observed pattern underscores the substantial influence of Grashof numbers on flow dynamics across different inclinations. Understanding this correlation is essential for comprehending how variations in the Grashof number distinctly affect and potentially regulate flow behaviors within various system configurations and inclinations.

### Figure 4

Figure 5 illustrates the impact of velocity ( $v$ ) across a range of Grashof numbers at a  $30^\circ$  inclination. The visualization reveals a direct relationship: as the Grashof number rises, velocity also increases proportionally. Both diagrams consistently show that higher Grashof numbers lead to increased velocity within the system. This pattern highlights the significant role of the Grashof number in affecting flow dynamics at various inclinations. Understanding this correlation is crucial for comprehending how variations in the Grashof number influence and potentially control flow behaviors in different system configurations and inclinations.

Both diagrams consistently demonstrate that as the Grashof number escalates, the velocity within the system also increases. This pattern emphasizes the significant influence of Grashof numbers on flow dynamics at varying inclinations. Understanding this



correlation is pivotal for grasping how changes in the Grashof number impact and potentially govern flow behaviors within different system configurations and inclinations.

Figure 5

In Table 1, the relationship between various variables and their influence on local skin friction is outlined. It's observed that  $Pr$ ,  $Sc$ , and inclination  $\alpha$  are associated with an upward trend in skin friction, indicating that changes in these factors lead to an increase in frictional forces experienced. Conversely,  $Gr$  and  $Gc$  show a contrasting impact, suggesting that as time progresses, alterations in these parameters result in a reduction in local skin friction. This distinction highlights the diverse effects these variables have on friction over time, with some causing an escalation and others a decline in this specific physical phenomenon.

Table 1

Table 2 illustrates the relationship between  $Sh$  and  $sc$  concerning time ( $t$ ). As  $Sh$  increases,  $Sc$  exhibits proportional growth. Meanwhile, as material transmission escalates, there is a concurrent increase in  $K_1^*$ .

Expanding on this, Table 2 demonstrates that changes in  $Sh$  directly impact the behavior of  $Sc, K_1^*$  concerning time. As  $Sh$  values rise, there is a consistent and proportional increase in  $Sc$  which indicates a close relationship between these two parameters. Simultaneously, the increase in material transmission coincides with a noticeable rise in  $K_1^*$  suggesting a correlation between the two factors. This table emphasizes how alterations in  $Sh$  and material transmission distinctly influence the dynamics of  $Sc, K_1^*$  over time.

Table 2

## CONCLUSION

The study examines the effects of a first-order chemical reaction on the linearly accelerated inclined isothermal plate, considering variable mass diffusion. The dimensionless equations are solved using the Laplace transform technique. The impact of velocity and concentration is analyzed for various physical parameters. The findings reveal

that the velocity increases as the phase angle  $\alpha^*$  and the chemical reaction parameter  $K_i$  decrease. Conversely, this trend is reversed with respect to time  $t$ . Additionally, it is observed that concentration increases as the chemical reaction parameter decreases. Skin friction increases with the Prandtl number (Pr) and the inclination angle, while it decreases over time with higher thermal and mass Grashof numbers (Gr and Gc). As the Sherwood number (Sh) rises, mass transfer increases proportionally.

## ACKNOWLEDGEMENT

The authors express their gratitude to the leadership at Panimalar Engineering College, Chennai, for their unwavering support throughout the execution of this research endeavor. Our institution has not provided any financial assistance or seed money to carry out the research work.

## Nomenclature

$A$	constant
$N^*$	species concentration in the fluid $mol / m^3$
$N_\infty^*$	species concentration away from the plate
$N_w^*$	species concentration near the plate
$B_1^*$	dimensionless concentration
$C_p$	specific heat at constant pressure $J.kg^{-1}.K^{-1}$
$D$	mass diffusion coefficient $m^2.s^{-1}$
$Gc$	Grashof number (mass)
$Gr$	Grashof number (thermal)
$g$	accelerated due to gravity $m.s^{-2}$
$k$	thermal conductivity $J.m^{-1}.K^{-1}$
$K_2^*$	Chemical reaction
$K_i$	Chemical reaction parameter
Pr	Prandtl number
$Sc$	Schmidt number
$Sh$	Sherwood number
$Nu$	Nusselt number

$F_w^*$	fluid temperature near the plate
$F_\infty^*$	Temperature away from the plate
$F^*$	fluid temperature closer to the plate
$t$	dimensionless time
$t_3^*$	time
$u$	fluid velocity in vertical direction $m.s^{-1}$
$u_0$	velocity of the plate $m.s^{-1}$
$P_2^*$	dimensionless velocity
$x$	spatial coordinate along the plate
$y'$	coordinate axis normal to the plate $m$
$y$	dimensionless coordinate axis normal to the plate
$Z_2^*$	similarity parameter

### Greek symbols

$\alpha^*$	Angle of inclination
$\beta_2$	volumetric coefficient of thermal expansion $K^{-1}$
$\beta_3^*$	volumetric coefficient of expansion with concentration $K^{-1}$
$\nu$	kinematic viscosity $m^2.s^{-1}$
$\rho$	density of the fluid $kg.m^{-3}$
$\tau$	dimensionless skin-friction $kg.m^{-1}.s^2$
$\sigma^*$	dimensionless temperature
<i>erfc</i>	complementary error function

### Subscripts

$w$	conditions at the wall
$\infty$	conditions in the free stream

### REFERENCES

1. O.A. Bég, T.A. Bég, A.Y. Bakier, V.R. Prasad, Int. J. Appl. Math. Mech. 5(2) (2009) 39–57. <https://www.scirp.org/reference/referencespapers?referenceid=207616>

2. O. Aydm, A. Kaya, Heat Mass Transfer 46 (2009) 129–136. <https://scihub.wf/10.1007/s00231-009-0551-4>
3. R. Muthucumaraswamy, G. Nagarajan, V.S.A. Subramanian, Ann. Fac. Eng. Hunedoara 8 (2010) 220-225. <https://annals.fih.upt.ro/pdf-full/2010/ANNALS-2010-3-45.pdf>
4. R. Muthucumaraswamy, Chem. Ind. Chem. Eng. Q. 16 (2010) 167–173. <https://doi.org/10.2298/CICEQ091231024M>
5. V. Bisht, M. Kumar, Z. Uddin, J. Appl. Fluid Mech. 4 (2011) 59–63. <https://doi.org/10.36884/jafm.4.04.11947>
6. M. Sundar Raj, R. Muthucumaraswamy, V.S.A. Subramanian, Int. J. Appl. Mech. Eng. 16(3) (2011) 885-891. <https://www.infona.pl/resource/bwmeta1.element.baztech-article-BPZ5-0017-0038>
7. O.D. Makinde, ZNA 67a (2012) 239–247. <https://doi.org/10.5560/zna.2012-0014>
8. P. Rana, R. Bhargava, O.A. Béq, Comput. Math. Appl. 64 (2012) 2816–2832. <https://doi.org/10.1016/j.camwa.2012.04.014>
9. M.S. Alam, M. Ali, M.D. Delowar Hossain, Int. J. Eng. Sci. 2(7) (2013) 81–88. <https://www.theijes.com/papers/v2-i7/Part.6/K0276081088.pdf>
10. R. Muthucumaraswamy, L. Jeyanthi, ARPN J. Eng. Appl. Sci. 10(20) (2015) 9596-9603 [http://www.arpnjournals.org/jeas/research\\_papers/rp\\_2015/jeas\\_1115\\_2914.pdf](http://www.arpnjournals.org/jeas/research_papers/rp_2015/jeas_1115_2914.pdf)
11. M. Narahari, S. Tippa, R. Pendyala, M.Y. Nayan, Recent Adv. Appl. Theor. Mech., Proc. WSEAS Int. Conf. (MECHANICS '15), 11<sup>th</sup>, 126–137 (2015). <http://www.wseas.us/e-library/conferences/2015/Malaysia/APTHME/APTHME-15.pdf>
12. H. Mondal, D. Pal, S. Chatterjee, P. Sibanda, Ain Shams Eng. J. 8 (2016) 2111–2121. <https://doi.org/10.1016/j.asej.2016.10.015>
13. Farjana Akter, Md. Manjiul Islam, Ariful Islam, Md. Shakhaoath Khan, Md. Saddam Hossain, Open Journal of Fluid Dynamics. 6 (2016) 62-74. <http://dx.doi.org/10.4236/ojfd.2016.61006>
14. Jyotsna Rani Pattnaik, Gouranga Charan Dash, Suprava Singh, Ain Shams Engineering Journal. 8(1) (2017) 67-75 <http://dx.doi.org/10.1016/j.asej.2015.08.014>
15. S. Khalid, M.A. Kamal, U. Rasheed, S. Farooq, S. Kussain, H. Waqas, J. Appl. Environ. Biol. Sci. 7(5) (2017) 154–165. [https://www.textroad.com/pdf/JAEBS/J.%20Appl.%20Environ.%20Biol.%20Sci.,%207\(5\)154-165,%202017.pdf](https://www.textroad.com/pdf/JAEBS/J.%20Appl.%20Environ.%20Biol.%20Sci.,%207(5)154-165,%202017.pdf)
16. S.V. Sailaja, B. Shanker, R. Srinivasa Raju, J. Nanofluids 6(3) (2017) 420-435. <https://doi.org/10.1166/jon.2017.1337>

17. R.K. Dhal, B. Jena, P.M. Sreekumar, *Int. Res. J. Adv. Eng. Sci.* 2(2) (2017) 299-303.  
<http://irjaes.com/wp-content/uploads/2020/10/IRJAES-V2N2P239Y17.pdf>
18. U.S. Rajput, Gaurav Kumar, *Jordanian J. Mech. Ind. Eng.* 11(1) (2017) 41-49.  
<https://jjmie.hu.edu.jo/vol%2011-1/JJMIE-13-16-01.pdf>
19. S. Agarwalla, N. Ahmed, *Heat Transfer-Asian Res.* (2017) 1-15. <https://sci-hub.wf/10.1002/htj.21288>
20. H. Mondal, D. Pal, S. Chatterje, P. Sibanda, *Ain Shams Eng. J.* 9(4) (2018) 2111-2121.  
<https://doi.org/10.1016/j.asej.2016.10.015>
21. M. Ahmad, M.A. Imran, M. Aleem, I. Khan, *J. Therm. Anal. Calorim.* 137 (2019) 1783 – 1796. <https://doi.org/10.1007/s10973-019-08065-3>
22. A. Sandhya, G.V. RamanaReddy, G.V.S.R. Deekshitulu, *Int. J. Appl. Mech. Eng.* 25 (3) (2020) 86-102. <https://doi.org/10.2478/ijame-2020-0036>
23. T.L. Oyekunle, S.A. Agunbiade, Oyekunle, A. Gunbiade, *J. Egypt. Math. Soc.* 28(51) (2020) 1-19. <https://doi.org/10.1186/s42787-020-00110-7>
24. S. ThamizhSuganya, P. Balaganesan, L. Rajendran, M. Abukhaled, *Eur. J. Pure Appl. Math.* 13(3) (2020). <https://doi.org/10.29020/nybg.ejpam.v13i3.3730>
25. A.S. Idowu, B.O. Falodun, *Arab. J. Basic Appl. Sci.* 27(1) (2020) 149–165.  
<https://doi.org/10.1080/25765299.2020.1746017>
26. M.B. Riaz, A. Atangana, S.T. Saeed, in *Fractional Order Analysis: Theory, Methods and Applications*, H. Dutta, A.O. Akdemir, A. Atangana, Eds., John Wiley & Sons Inc., (2020) 253–282. <https://sci-hub.se/https://doi.org/10.1002/9781119654223.ch10>
27. P.K. Dadheech, P. Agrawal, A. Sharma, A. Dadheech, Q. Al-Mdallal, S.D. Purohit, *Case Stud. Therm. Eng.* 28 (2021) 101491. <https://doi.org/10.1016/j.csite.2021.101491>
28. A.A. Zafar, J. Awrejcewicz, G. Kudra, N.A. Shah, S.-J. Yook, *Case Stud. Therm. Eng.* 27 (2021) <https://doi.org/10.1016/j.csite.2021.101249>
29. D.P.C. Rao, S. Thiagarajan, V. Srinivasakumar, *Heat Transfer* 50 (7) (2021) 7120-7138.  
<https://onlinelibrary.wiley.com/doi/10.1002/htj.22220>
30. K. Raghunath, N. Gulle, R.R. Vaddemani, O. Mopuri, *Heat Transfer* 51(3) (2021) 2742-2760 <https://onlinelibrary.wiley.com/doi/10.1002/htj.22423>
31. R. Vijayaragavana, V. Bharathib, J. Prakash, *Indian J. Pure Appl. Phys.* 59 (2021) 28-39.  
<https://pdfs.semanticscholar.org/7d14/5f4f87013207ba593f8d93ed60d2030d028d.pdf>
32. C. PavanKumar, K. Raghunath, M. Obulesu, *Turk. J. Comp. Math. Edu.* 12(13) (2021) 960-977. <https://turcomat.org/index.php/turkbilmate/article/view/8584/6710>

33. R. SureshBabu, T. SaravanKumar, M.V. Govindaraju, B. Mallikarjuna, *Biointerface Res. Appl. Chem.* 11(5) (2021) 13252-13267.  
<https://doi.org/10.33263/BRIAC115.1325213267>
34. Raghunath Kodi, Obulesu Mopuri, *Heat Transfer* 51 (2021) 733-752  
<https://doi.org/10.1002/htj.22327>
35. S.G. Bejawada, W. Jamshed, R. Safdar, Y.D. Reddy, M.M. Alanazi, H.Y. Zahran, M.R. Eid, *Coatings* 12(2) (2022) 151. <https://doi.org/10.3390/coatings12020151>
36. H.I. Osman, N.F.M. Omar, D. Vieru, Z. Ismail, *J. Adv. Res. Fluid. Mech. Therm. Sci.* 92(1) (2022) 18-27. <https://doi.org/10.37934/arfmts.92.1.1827>
37. B.K. Tad, N. Ahmed, *Biointerface. Res. Appl. Chem.* 12(5) (2022) 6280-6296.  
<https://biointerfaceresearch.com/wp-content/uploads/2021/11/20695837125.62806296.pdf>
38. G. Nagarajan, M. SundarRaj, R. Muthucumaraswamy, *Int. J. Appl. Mech. Eng.* 27(4) (2022) 105-116. <https://doi.org/10.2478/ijame-2022-0053>
39. B.C. Nhial, V.S. HariBabu, V.N. Vellanki, G.Y. Sagar, *JPSP* 6(5) (2022) 697–706.  
<https://journalppw.com/index.php/jpsp/article/view/5861/3858>
40. K. Raghunath, N. Gulle, R. R. Vaddemani, O. Mopuri, *Heat Transfer* 51(3) (2022) 2742-2760. <https://doi.org/10.1002/htj.22423>
41. R. MohanaRamana, K. VenkateswaraRaju, K. Raghunath, *Heat Transfer* 51(7) (2022) 6431-6449. <https://doi.org/10.1002/htj.22598>
42. N. Shehzad, A. Zeeshan, M. Shakeel, R. Ellahi, S. M. Sait, *Coatings* 12(430) (2022) 1-25. <https://doi.org/10.3390/coatings12040430>
43. A. Raza, U. Khan, Z. Raizah, S.M. Eldin, A.M. Alotaibi, S. Elattar, A.M. Abed, *Symmetry* 14 (2022) 2412. <https://www.mdpi.com/2073-8994/14/11/2412>
44. P. Sivakumar, R. Muthucumaraswamy, *Gis Sci. J.* 9(1) (2022) 167-177. 1869-9391.  
[https://drive.google.com/file/d/1DKDzhYzeHz1QWap1sh\\_dTcDFXAfyyvDI-/view](https://drive.google.com/file/d/1DKDzhYzeHz1QWap1sh_dTcDFXAfyyvDI-/view)
45. K. Raghunath, O. Mopuri, *Heat Transfer*, 51 (2022), 733-752.  
<https://doi.org/10.1002/htj.22327>
46. M. SundarRaj, G. Nagarajan, V.P. Murugan, R. Muthucumaraswamy, *Int. J. Appl. Mech. Eng.* 28(2) (2023) 64-76. <https://www.ijame-poland.com/pdf-168439-91810?filename=Impacts%20of%20chemical.pdf>
47. N.S. Wahid, N.M. Arifin, N.S. Khashi, I. Pop, *Alexandria Eng. J.* 66 (2023) 769–783.  
<https://doi.org/10.1016/j.aej.2022.10.075>
48. J.S. Huang, *Journal of Mechanics*, 39(2023) 88-104 <https://doi.org/10.1093/jom/ufad006>

49. B. Prabhakar Reddy, M.H. Simba, Alfred Hugo, Hindawi International Journal of Chemical Engineering. Article ID 9342174 (2023) <https://doi.org/10.1155/2023/9342174>
50. K.V. Raju, R. Mohanaramana, S. Sudhakar Reddy, K. Raghunath, Communications in Mathematics and Applications. 14(1) (2023) 237-255 <https://doi.org/10.26713/cma.v14i1.1867>
51. R. Rajaraman, R. Muthucumaraswamy, Chem. Ind. Chem. Eng. Q. 30 (3) 223-230 (2024) <https://doi.org/10.2298/CICEQ230526025R>

**Figure captions:**

Figure 1 Concentration profile for ‘K’

Figure 2 Velocity profiles for different values of ‘t’: a)  $\alpha=\pi/3$ ,  $k=10, Pr=0.71, Sc=0.6, Gr=5, Gc=15$ ; b)  $\alpha = \pi/4$ ,  $k=10, Pr=0.71, Sc=0.16, Gr=10, Gc=5$

Figure 3 Velocity profiles for different values of ‘K’: a)  $\alpha=\pi/4$ ,  $t=0.8, Pr=0.71, Sc=0.16, Gr=15, Gc=15$ ; b)  $\alpha=\pi/6$ ,  $t=0.2, Pr=0.71, Sc=0.3, Gr=15, Gc=15$ ; c)  $\alpha=\pi/6$ ,  $t=0.4, Pr=0.71, Sc=0.16, Gr=5, Gc=5$

Figure 4: Velocity profiles for different values of ‘Gc’: a)  $\alpha=\pi/3$ ,  $k=5, t=0.4, Pr=0.71, Sc=0.16, Gr=5$ ; b)  $\alpha = \pi/6$ ,  $k=10, t=0.6, Pr=0.71, Sc=0.16, Gr=5$

Figure5: Velocity profiles for different values of ‘Gr’: a)  $\alpha=\pi/6$ ,  $k=10, t=0.4, Pr=0.71, Sc=0.6, Gc=15$ ; b)  $\alpha = \pi/3$ ,  $k=5, t=0.4, Pr=0.71, Sc=0.16, Gc=5$

**Table 1** Skin friction values for various parameters

$\alpha$ (in deg)	$t$	$Gr$	$Gc$	sc	pr	$K'_1$	$\tau$
30	0.6	2	2	0.16	7	2	5.9457
60	0.8	5	2	0.16	0.71	2	5.6004
60	0.6	5	5	0.3	0.71	2	5.4963
30	0.2	2	5	0.3	7	10	4.6919
45	0.2	2	5	0.6	0.71	5	4.5596
45	0.2	5	5	0.6	0.71	5	3.9786
60	0.2	5	10	0.3	7	5	2.5862
45	0.4	2	2	0.16	7	5	1.5473
60	0.4	5	2	0.16	0.71	5	0.1611
30	0.4	5	2	0.16	0.71	2	-3.3517



**Table 2** Sherwood number for various parameters

t	sc	$K_2^*$	Sh
0.2	0.6	10	0.5502
0.2	0.6	5	0.4396
0.4	0.16	5	0.4293
0.6	0.16	2	0.4866
0.8	0.3	10	1.4631
0.6	0.3	10	1.1066
0.8	2.01	5	2.8177
0.4	2.01	2	1.0824
0.6	2.01	5	2.1432
0.2	0.3	5	0.3244

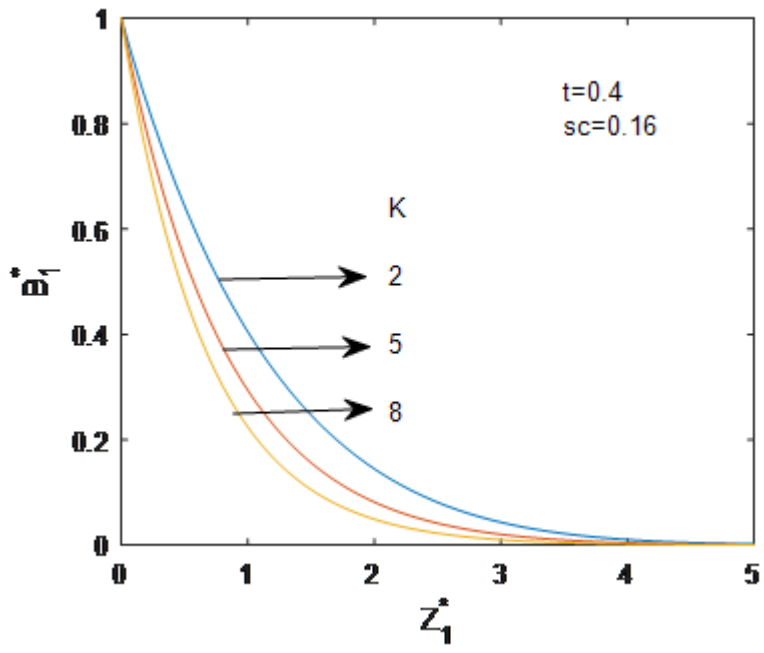


Figure 1

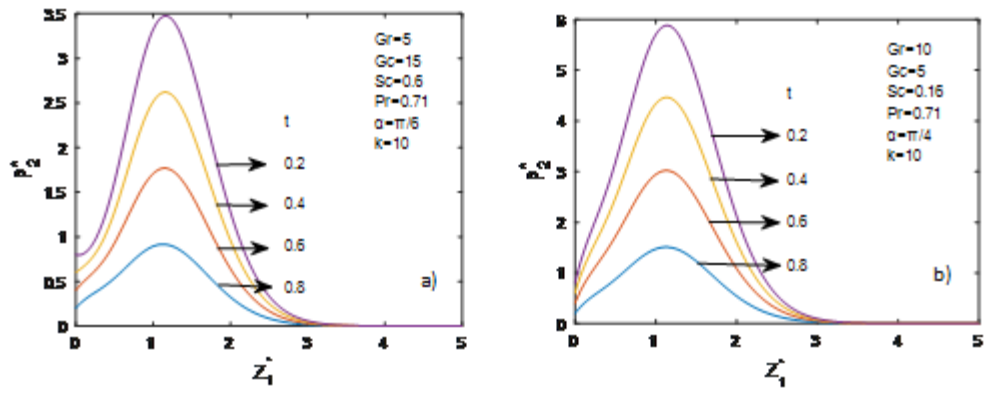


Figure 2

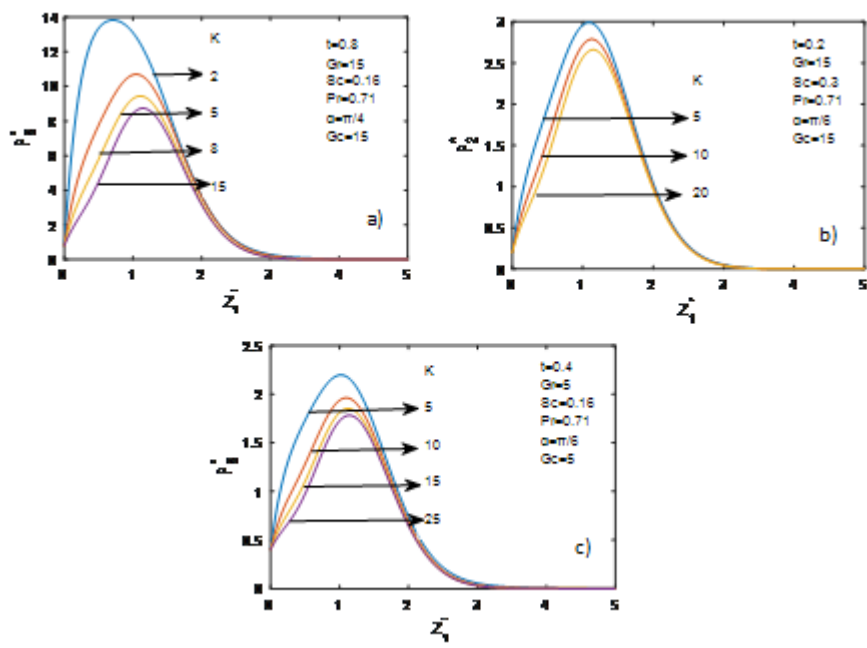


Figure 3

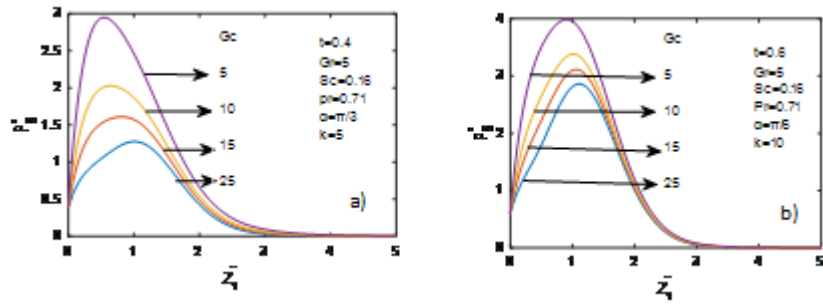


Figure 4

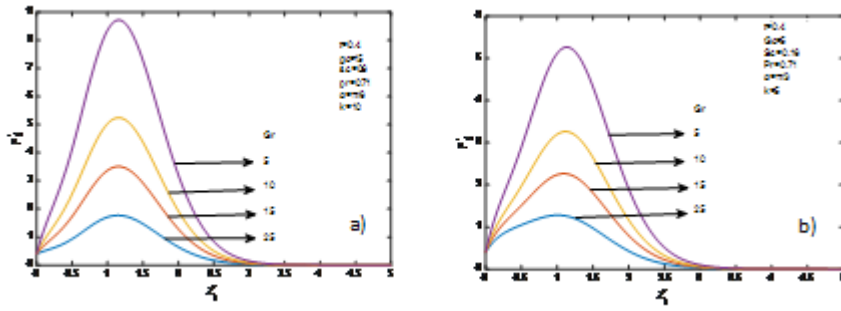


Figure 5